ACS Chemical Neuroscience

Research Article

pubs.acs.org/chemneuro

Synthesis and Imaging Validation of [^{18}F]MDL100907 Enabled by Ni-Mediated Fluorination

Hong Ren,[†,‡] Hsiao-Ying Wey,[†] Martin Strebl,[‡] Ramesh Neelamegam,[†] Tobias Ritter,*[,‡] and Jacob M. Hooker*[,†]

[†]Athinoula A. Martinos Center for Biomedical Imaging, Massachusetts General Hospital and Harvard Medical School, 13th Street, Charlestown, Massachusetts 02129, United States

[‡]Department of Chemistry and Chemical Biology, Harvard University, 12 Oxford Street, Cambridge, Massachusetts 02138, United States

Supporting Information

ABSTRACT: Several voids exist in reliable positron emission tomography (PET) radioligands for quantification of the serotonin (5HT) receptor system. Even in cases where 5HT radiotracers exist, challenges remain that have limited the utility of 5HT imaging in clinical research. Herein we address an unmet need in 5HT$_{2a}$ imaging using innovative chemistry. We report a scalable and robust synthesis of [^{18}F]-MDL100907, which was enabled by a Ni-mediated oxidative fluorination using [^{18}F]fluoride. This first demonstration of a Ni-mediated fluorination used for PET imaging required development of a new reaction strategy that ultimately provided high specific activity [^{18}F]MDL100907. Using the new synthetic strategy and optimized procedure, [^{18}F]MDL100907 was evaluated against [^{11}C]MDL100907 for reliability to quantify 5HT$_{2a}$ in the nonhuman primate brain and was found to be superior based on a single scan analysis using the same nonhuman primate. The use of this new 5HT$_{2a}$ radiotracer will afford clinical neuroscience research the ability to distinguish 5HT$_{2a}$ receptor abnormalities binding between healthy subjects and patients even when group differences are small.

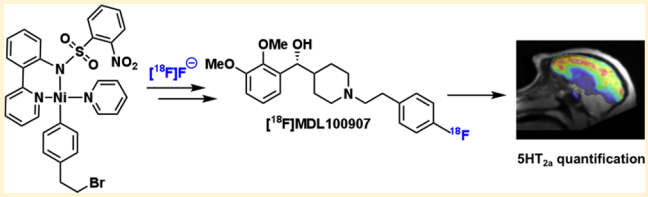

KEYWORDS: *[^{18}F]flourination, nickel-mediated, serotonin receptors, 5HT$_{2a}$, MDL100907, PET imaging*

Serotonin 2a receptors (5HT$_{2a}$) are implicated in the pathophysiology of a number of neuropsychiatric disorders. A large body of literature suggests that dysfunction of 5HT$_{2a}$ may be related or contribute to schizophrenia,[1] major depressive disorder,[2] and bipolar disorder,[3] among others. To quantify 5HT$_{2a}$ receptors in the human brain, there have been major efforts to develop a selective radioligand for use in positron emission tomography (PET). Several radiotracers have been developed, of which [^{18}F]altanserin and [^{11}C]-MDL100907 (Figure 1) have proven to be most useful to date for studying 5HT$_{2a}$ dysregulation in disease. Neither of these ligands is ideal. For example, despite great selectivity and affinity, [^{18}F]altanserin is metabolized rapidly and the resulting radiometabolites penetrate the blood-brain barrier.[4] The presence of radiometabolites in the brain complicates quantification of [^{18}F]altanserin binding and has hindered its broad adoption in neuroscience research. [^{11}C]MDL100907 also exhibits excellent selectivity and affinity to 5HT$_{2a}$ receptors and without the potential signal confound by brain penetrant radiometabolites.[5] However, a major drawback of [^{11}C]-MDL100907 is that its short half-life (20.4 min) does not match the pharmacokinetic and biological half-life of the radiotracer. The mismatch of the isotope and biological half-life makes it difficult to measure [^{11}C]MDL100907 binding during late time points (>90 min) where the ligand is approaching an equilibrium between blood and tissue. Using earlier time points introduces errors in distribution volume and binding potential estimates that are on the order of potential biological effect size or group differences.[6]

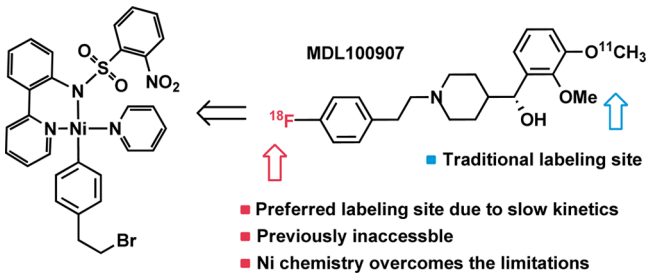

Figure 1. MDL 100907, a highly selective antagonist for imaging 5HT$_{2a}$ receptors.

The mismatch between biological and isotope half-life for [^{11}C]MDL100907 can be avoided due to the fact that MDL100907 contains an aryl fluoride that could be substituted with fluorine-18 ($t_{1/2}$ = 109.8 min). Thus, the use of

Received: April 11, 2014
Revised: May 20, 2014
Published: May 20, 2014

[^{18}F]MDL100907 has been suggested and attempted.[7] However, synthesis of [^{18}F]MDL100907 is not trivial given that the aryl fluoride is on an electron-rich ring.

Methods to activate the arene for nucleophilic aromatic substitution have had modest success (e.g., through the use of iododium salt precursor).[8] All attempts to date have failed to deliver a fluorination method that enables the comparison of [^{18}F]MDL100907 to [^{11}C]MDL100907 in the nonhuman primate brain as a stepping stone to human use for [^{18}F]MDL100907. Here, we report a scalable, robust synthesis of [^{18}F]MDL100907 using a Ni-mediated oxidative fluorination strategy with [^{18}F]fluoride and demonstrate [^{18}F]MDL100907 provides superior $5HT_{2a}$ distribution/density estimates to [^{11}C]MDL100907.

In our initial report of Ni-mediated fluorination, aqueous [^{18}F]fluoride obtained from cyclotron was used for the reaction.[9] Using 5 μL of [^{18}O]H_2O (1% of the reaction volume), we achieved good aryl [^{18}F]fluoride labeling in less than 1 min at room temperature. However, two chemical constraints (somewhat related) limited our initial radioactive scale-up attempts. First, a simple increase in the volume of [^{18}F]fluoride−water added to the Ni-mediated reaction, above 1% v/v, competitively degraded the Ni complex and oxidant. Given that [^{18}F]fluoride is produced by irradiation of 2.4 mL of [^{18}O]water, aqueous incompatibility limited our overall isolable yield to a maximum of 0.2% (5 μL/2.4 mL). Second, initial attempts to remove water under classic radiochemistry conditions provided dry [^{18}F]fluoride in solutions that were too basic and resulted in poor radiochemical labeling reactions with the Ni-complex and oxidant (Scheme 1A).

RESULTS AND DISCUSSION

Efforts were taken to overcome the incompatibility of Ni-mediated [^{18}F]fluorinations with basic conditions to facilitate the use of the Ni-method in a scalable process for PET imaging. A number of bases were screened to determine if reducing the basicity of the solution would be sufficient for scale-up (Scheme 1). Bases such as potassium or cesium oxalate (pK_{a2} = 4.27), potassium bicarbonate (pK_{a1} = 6.35), and potassium hydrogen phosphate (pK_{a2} = 7.21) provided efficient elution of [^{18}F]fluoride from the ion exchange cartridge and were sufficiently basic (relative to HF) to prevent the loss of [^{18}F]fluoride during azeotropic drying (performed at 108 °C), but each failed to provide a highly soluble [^{18}F]fluoride in acetonitrile for the Ni-mediated reaction (Scheme 1B, entries 1, 4, and 6). When phase transfer agents could be used to improve [^{18}F]fluoride solubility, the basicity of the reaction solution increased accordingly and thus eroded the radiochemical conversion (RCC). For example, [^{18}F]fluoride solubility could be improved using tetrabutylammonium bicarbonate (TBAB), but the resulting radiochemical conversion was <1% (Scheme 1B, entry 8). For scale-up, it was important to optimize all aspects of the reaction process. Thus, we envisioned that an in-process pH adjustment might overcome the adverse effect of excess base if a suitable organic buffer could be identified as compatible with the Ni-mediated [^{18}F]fluorination protocol. To this end, a series of weak organic acids were added to effectively produce a bicarbonate buffer in which the Ni-mediated [^{18}F]fluorination would proceed. Ultimately, we settled on pyridinium *p*-toluenesulfonate (PPTS) as the buffering acid with TBAB as the elution base (Scheme 1B, entry 9).

Scheme 1. Development of Optimized Ni-Mediated [^{18}F] Fluorination Process[a]

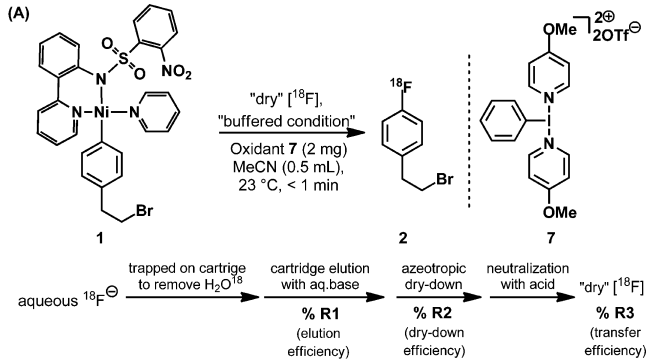

(B)

Entry	*Base*	*%R_1*	*% R_2*	*%R_3*	*Acid*	*%RCC*
1	$Cs_2C_2O_4$/ 18-cr-6	92	93	28	-	15
2	$Cs_2C_2O_4$/ 24-cr-8	91	90	30	-	13
3	Cs_2CO_3/ 18-cr-6	94	92	23	-	11
4	$KHCO_3$/ 18-cr-6	90	86	28	-	14
5	K_3PO_4/ 18-cr-6	97	96	17	-	9
6	K_2HPO_4 18-cr-6	92	93	19	-	13
7[a]	TBAB	51	82	60	-	21
8[b]	TBAB	89	90	55	-	<1
9[b]	TBAB	90	87	57	PPTS	35
10[b]	TBAB	90	89	61	LPTS	21
11[b]	TBAB	91	89	64	CH_3COOH	25

[a](A) Typical chemical process in fluorine-18 chemistry. (B) Development of a globally optimal Ni-mediated [^{18}F]fluorination (18-cr-6:18-crown-6 ether; 24-cr-8:24-crown-8 ether; TBAB, tetrabutylammonium bicarbonate).

The use of PPTS enabled the successful synthesis of the previously inaccessible radiotracer [^{18}F]MDL100907 with high specific activity according to Scheme 2. The labeling precursor **1** was synthesized from commercially available 1-bromo-4-(2-bromoethyl)benzene **3** in two steps. Oxidative addition furnished a nickel intermediate **4** in 73% yield, which then

Scheme 2. Automated Radiosynthesis of [^{18}F]MDL100907

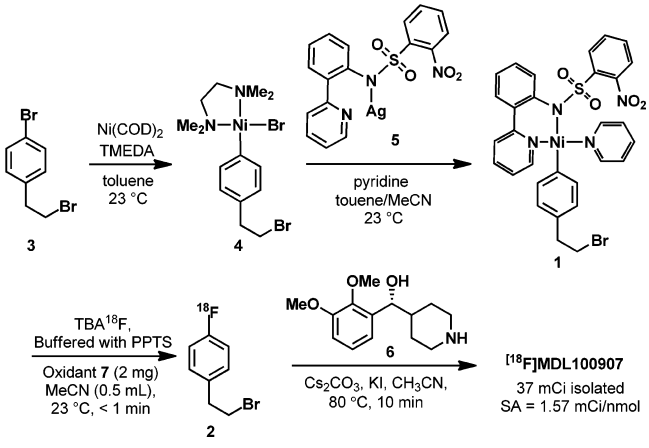

dx.doi.org/10.1021/cn500078e | ACS Chem. Neurosci. 2014, 5, 611−615

underwent transmetalation with (2-(2-pyridinyl)phenyl-2-nitrobenzenesulfonamide)silver(I) **5** to afford the desired labeling precursor **1** in 51% yield. Radiosynthesis was achieved using a simple one-pot, two step automated method. After azeotropic drying and addition of PPTS (in MeCN) using a Siemens GN reactor, [^{18}F]1-(2-bromoethyl)-4-fluorobenzene **2** was produced in less than 1 min and immediately treated with excess chiral amine **6.** The crude reaction mixture was diluted with water and purified by reverse-phase semipreparative HPLC, which afforded 37 mCi for dose reformulation. [^{18}F]MDL100907 was obtained in a sterile, 10% ethanol/90% saline (v/v) solution after reformulation in an overall nondecay corrected yield of 3% (1.57 mCi/nmol at TOI).

With [^{18}F]MDL100907 in hand, we compared its brain uptake and pharmacokinetic with [^{11}C]MDL100907. To accomplish this, we produced and administered [^{11}C]-MDL100907 (5.05 mCi, 1.53 mCi/nmol) to a *Papio anubis* baboon. After an imaging and decay time of 2.5 h, [^{18}F]MDL100907 (5.11 mCi, 1.57 mCi/nmol) was administered to the same animal for direct intrasubject comparison. [^{18}F]MDL100907 showed high uptake in the cortex and subcortical regions, similar to [^{11}C]MDL100907 (Figure 2).

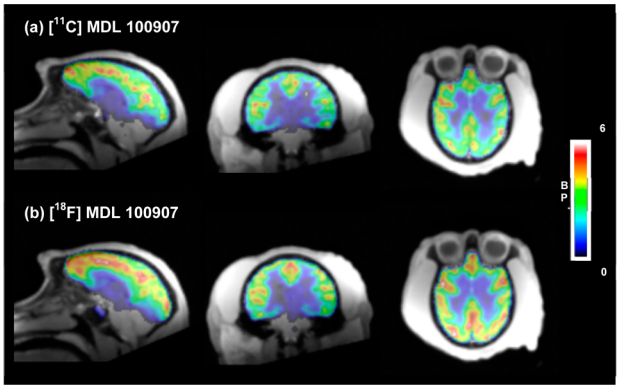

Figure 2. Voxel-wise binding potential (BP_{ND}) maps of (a) [^{11}C]MDL100907 (90 min) and (b) [^{18}F]MDL100907 (120 min) overlaid on structural MRI.

The concentration of [^{18}F]MDL100907 reached maximum at ~40 min postradiotracer injection with washout kinetics nearly identical to that of [^{11}C]MDL100907 (Figure 3a and b). Although it is a potential concern that the radiometabolites of [^{18}F]MDL100907 could be brain-penetrant, regional [^{11}C]-MDL100907 and [^{18}F]MDL100907 time−activity curves (TACs) show similar characteristics, implying that no radiometabolite was accumulating with [^{18}F]MDL100907 (Figure 3a and b).

However, to more rigorously compare the quantification of $5HT_{2a}$ binding for each radiotracer, both the Logan reference tissue model and the modified simplified reference tissue model (SRTM2) were applied to obtain estimates of specific binding (BP_{ND}).[10] Kinetic analysis methods including compartmental models with arterial input function and reference tissue models have been carefully examined and compared for [^{11}C]-MDL100907 in human subjects. The Logan plot was recommended to be the most reliable method for both regional and voxel-wise analysis.[11] [^{11}C]MDL100907 BP_{ND} quantified using Logan plot and SRTM2 are positively correlated (see Supporting Information Figure S7, R^2 = 0.99, Spearman r = 0.97, $p < 0.0001$) indicating both methods generate comparable

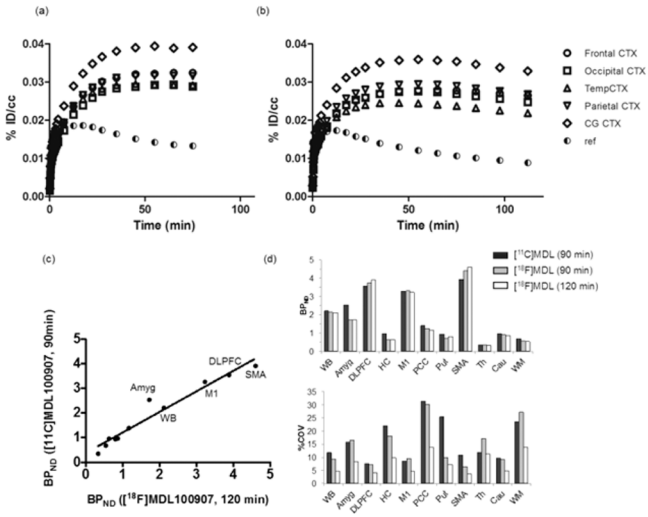

Figure 3. (a) Time−activity curve of [^{11}C]MDL100907 (90 min scan). (b) Time−activity curve of [^{18}F]MDL100907 (120 min scan). (c) Correlation analysis, Spearman r = 0.98 ($p < 0.0001$), R^2 = 0.95. (d) Comparison of regional binding potential (BP_{ND}) and percent coefficient of variation (%COV) of the fitting derived from [^{11}C]MDL100907 (90 min) and [^{18}F]MDL100907 (90 and 120 min) PET data using the modified simplified reference tissue model (SRTM2). (WB, whole brain; Amyg, amygdala; DLPFC, dorsolateral prefrontal cortex; HC, habenular commissure; M1, primary motor cortex; PCC, posterior cingulate; Put, putamen; SMA, supplementary motor area; Th, thalamus; Cau, caudate nucleus; WM, white matter.)

results. To compare the performance of [^{11}C]MDL100907 and [^{18}F]MDL100907 for kinetic analysis, the SRTM2 was applied to estimate BP_{ND} and percent coefficient of variation (COV) of the fits on [^{11}C]MDL100907 (90 min), [^{18}F]MDL100907 (90 min), and [^{18}F]MDL100907 (120 min). Percent COV represents the standard error of the fitting procedure. Regional BP_{ND} as well as the %COV of the fits were compared and are plotted in Figure 3d. Quantitative BP_{ND} values were comparable between the [^{11}C]MDL100907 and [^{18}F]-MDL100907 (90 and 120 min) (Figure 3d) and were positively correlated (Figure 3c, R^2 = 0.95, Spearman r = 0.98, $p < 0.0001$). However, based on the single scan analysis using the same nonhuman primate, [^{18}F]MDL100907 with 120 min scan duration generates the most robust fitting results as indicated by the smallest %COV within the same brain region (Figure 3d).

These results suggest that the prolonged scan time enabled by [^{18}F]MDL100907 might allow more reliable quantification of $5HT_{2a}$ receptors for certain brain related diseases where the effect size of $5HT_{2a}$ receptor binding may be small between healthy subjects and patients.[12] When comparing [^{11}C]-MDL100907 and [^{18}F]MDL100907 with the same scan length (90 min), [^{18}F]MDL100907 data also showed smaller %COV and smaller weighted residuals of the fittings than those of [^{11}C]MDL100907 in the majority of brain regions examined (Figure 3d). Taken together, [^{18}F]MDL100907 outperformed [^{11}C]MDL100907, most likely due to a better noise characteristic because of less decay and thus higher count rates. [^{18}F]MDL100907 also enables a longer scan to be obtained, which may help stabilize outcome measurements due to the slow pharmacokinetics of radiolabeled MDL100907. Although not significantly different, regional BP_{ND} values and voxel-wise BP_{ND} maps show higher BP_{ND} derived from [^{18}F]MDL100907 than those derived from [^{11}C]MDL100907 in high binding

dx.doi.org/10.1021/cn500078e | *ACS Chem. Neurosci.* 2014, 5, 611−615

regions such as the frontal cortex (DLPFC) and supplementary motor area (SMA), but lower BP_{ND} in low binding regions such as thalamus, caudate, and putamen (Figures 2 and 3). This discrepancy based on our initial study could result from the lower noise level at late time points of [^{18}F]MDL100907 data that drives the fitting results, and may represent a more accurate measurement. Figure 4 shows a smaller fitting residual

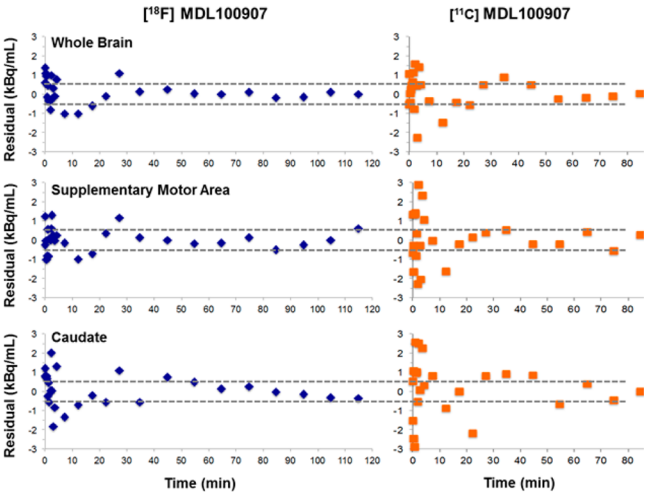

Figure 4. Residual of the kinetic model fitting using the modified simplified reference tissue model (SRTM2) from the whole brain, supplementary motor area, and caudate regions of interest.

of [^{18}F]MDL100907 than [^{11}C]MDL100907 when comparing the same time points, which further corroborates a better noise characteristic of [^{18}F]MDL100907. With replicate scans and analyses, it is likely that [^{18}F]MDL100907 will prove superior to [^{11}C]MDL100907 in certain $5HT_{2a}$ imaging scenarios.

CONCLUSIONS

A scalable, robust synthesis of previously inaccessible [^{18}F]-MDL100907 was developed using a Ni-mediated oxidative fluorination strategy with [^{18}F]fluoride. Key to our success was the development of a simple, in-process pH adjustment/buffering strategy to overcome initial challenges with the Ni-mediated oxidative [^{18}F]fluorination. We prepared [^{18}F]-MDL100907 in high specific activity and compared it to [^{11}C]MDL100907 in the brain of a nonhuman primate. As demonstrated by our initial finding, [^{18}F]MDL100907 provides superior 5HT2a distribution/density estimates to [^{11}C]-MDL100907. Repetitive scans and analyses with [^{18}F]-MDL100907 are in progress to demonstrate the robustness of this method for translation to human imaging for clinical neuroscience research.

ASSOCIATED CONTENT

Supporting Information

Experimental details, including methods and synthesis, radiochemistry, baboon PET/MRI imaging, and data analysis; additional figures and spectroscopic data for compounds **1**, **4**, and **8**. This material is available free of charge via the Internet at http://pubs.acs.org.

AUTHOR INFORMATION

Author Contributions

H.R. developed the scalable Ni-mediated [^{18}F]fluorination process, synthesized [^{18}F]MDL100907 for nonhuman primate study and carried out preliminary PET imaging data analysis. H.-Y. W carried out PET imaging data analysis. M.S. assisted in synthesis of the labeling precursor 1. R.N. assisted in synthesis of [^{11}C]MDL100907. J.M.H. and T.R. conceived and directed the project. All authors contributed to the preparation and review of the manuscript.

Funding

H.R. and H.-Y.W. are supported by the Harvard/MGH Nuclear Medicine Training Program from the Department of Energy (DE-SC0008430). M.S. is supported by a training grant from the NIH Blueprint for Neuroscience Research (T90DA022759/R90DA023427). This research was carried out at the Athinoula A. Martinos Center for Biomedical Imaging at the Massachusetts General Hospital, using resources provided by the Center for Functional Neuroimaging Technologies, P41EB015896, a P41 Regional Resource supported by the National Institute of Biomedical Imaging and Bioengineering (NIBIB), National Institutes of Health. This work also involved the use of instrumentation supported by the NIH Shared Instrumentation Grant Program and/or High-End Instrumentation Grant Program; specifically, Grant Numbers: S10RR017208, S10RR026666, S10RR022976, S10RR019933, and S10RR029495.

Notes

The authors declare no competing financial interest.

ACKNOWLEDGMENTS

The authors are grateful to members of the Ritter lab who provided early support for this work, particularly Heejun Lee. Additionally, imaging work was supported by Martinos Center staff including Helen Deng, Shirley Hsu, Grae Arabsz, Judit Sore, and Nathan Schauer.

REFERENCES

(1) (a) Uçok, A., Alpsan, H., Cakir, S., and Saruhan-Direskeneli, G. (2007) Association of a serotonin receptor 2A gene polymorphism with cognitive functions in patients with schizophrenia. *Am. J. Med. Genet., Part B 144B*, 704−707. (b) Rasmussen, H., Erritzoe, D., Andersen, R., Ebdrup, B. H., Aggernaes, B., Oranje, B., Kalbitzer, J., Madsen, J., Pinborg, L. H., Baaré, W., Svarer, C., Lublin, H., Knudsen, G. M., and Glenthoj, B. (2010) Decreased frontal serotonin 2A receptor binding in antipsychotic-naive patients with first-episode schizophrenia. *Arch. Gen. Psychiatry 67*, 9−16. (c) Rasmussen, H., Ebdrup, B. H., Erritzoe, D., Aggernaes, B., Oranje, B., Kalbitzer, J., Pinborg, L. H., Baaré, W. F., Svarer, C., Lublin, H., Knudsen, G. M., and Glenthoj, B. (2011) Serotonin 2A receptor blockade and clinical effect in first-episode schizophrenia patients treated with quetiapine. *Psychopharmacology (Berlin, Ger.) 213*, 583−592.

(2) (a) Noro, M., Antonijevic, I., Forray, C., Kasper, S., Kocabas, N. A., Lecrubier, Y., Linotte, S., Mendlewicz, J., Montgomery, S., Snyder, L., Souery, D., Verbanck, P., Zohar, J., and Massat, I. (2010) 5HT1A and 5HT2A receptor genes in treatment response phenotypes in major depressive disorder. *Int. Clin. Psychopharmacol. 25*, 228−231. (b) G. Frank, G. K., Kaye, W. H., Meltzer, C. C., Price, J. C., Greer, P., McConaha, C., and Skovira, K. (2002) Reduced 5-HT2A receptor binding after recovery from anorexia nervosa. *Biol. Psychiatry 52*, 896−906. (c) Soloff, P. H., Price, J. C., Meltzer, C. C., Fabio, A., Frank, G. K., and Kaye, W. H. (2007) 5HT2A receptor binding is increased borderline personality disorder. *Biol. Psychiatry 62*, 580−587.

(3) (a) Lee, S. Y., Chen, S. L., Chang, Y. H., Chu, C. H., Huang, S. Y., Tzeng, N. S., Wang, C. L., Lin, S. H., Lee, I. H., Yeh, T. L., Yang, Y. K., and Lu, R. B. (2012) The ALDH2 and 5-HT2A genes interacted in bipolar-I but not bipolar-II disorder. *Prog. Neuropsychopharmacol. Biol. Psychiatry 38*, 247−251. (b) Choi, K. Y., Yoon, H. K., and Kim, Y. K. (2010) Association between serotonin-related polymorphisms in 5HT2A, TPH1, TPH2 genes and bipolar disorder in Korean population. *Psychiatry Invest. 7*, 60−66.

(4) Tan, P. Z., Baldwin, R. M., Van Dyck, C. H., Al-Tikriti, M., Roth, B., Khan, N., Charney, D. S., and Innis, R. B. (1999) Characterization of radioactive metabolites of 5-HT2A receptor PET ligand [^{18}F]-altanserin in human and rodent. *Nucl. Med. Biol. 26*, 601−608.

(5) (a) Ito, H., Nyberg, S., Halldin, C., Lundkvist, C., and Farde, L. (1998) PET Imaging of Central 5HT2A Receptors with Carbon-11-MDL 100,907. *J. Nucl. Med. 39*, 208−214. (b) Mathis, C. A., Mahmood, K., Huang, Y., Simpson, N. R., Gerdes, J. M., and Price, J. C. (1996) Synthesis and preliminary in vivo evaluation of [^{11}C]-MDL100907: a potent and selective radioligand for the 5HT2A receptor system. *Med. Chem. Res. 6*, 1−10.

(6) Vernaleken, I., Peters, L., Raptis, M., Lin, R., Buchholz, H., Zhou, Y., Winz, O., Rösch, F., Bartenstein, P., Wong, D., Schäfer, W., and Gründer1, G. (2011) The applicability of SRTM in [^{18}F]fallypride PET investigations: impact of scan durations. *J. Cereb. Blood Flow Metab. 31*, 1958−1966.

(7) Muhlhausen, U., Ermert, J., Herth, M. M., and Coenen, H. H. (2009) Synthesis, radiofluorination and first evaluation of (±)-[^{18}F]MDL 100907 as serotonin 5-HT2A receptor antagonist for PET. *J. Labelled Compd. Radiopharm. 52*, 6−12.

(8) (a) Pike, V. W., and Aigbirhio, F. I. (1995) Reactions of cyclotron-produced [^{18}F]fluoride with diaryliodonium salts—a novel single-step route to no-carrier-added [^{18}F]fluoroarenes. *J. Chem. Soc., Chem. Commun.*, 2215−2216. (b) Shah, A., Pike, V. W., and Widdowson, D. A. (1998) The synthesis of [18F]fluoroarenes from the reaction of cyclotron-produced [18F]fluoride ion with diaryliodonium salts. *J. Chem., Soc., Perkin Trans. 1*, 2043−2046. (c) Martin-Santamaria, S., Carroll, M. A., Carroll, C. M., Carter, C. D., Pike, V. W., Rzepa, H. S., and Widdowson, D. A. (2000) Fluoridation of heteroaromatic iodonium salts—experimental evidence supporting theoretical prediction of the selectivity of the process. *Chem. Commun.*, 649−650. (d) Chun, J.-H., Lu, S., and Pike, V. W. (2011) Rapid and efficient radiosyntheses of meta-substituted [^{18}F]fluoroarenes from [^{18}F]fluoride ion and diaryliodonium tosylates within a microreactor. *Eur. J. Org. Chem.*, 4439−4447.

(9) Lee, E., Hooker, J. M., and Ritter, T. (2012) Nickel-mediated oxidative fluorination for PET with aqueous [^{18}F] fluoride. *J. Am. Chem. Soc. 134*, 17456−17458.

(10) Logan, J. (2000) Graphical analysis of PET data applied to reversible and irreversible tracers. *Nucl. Med. Biol. 27*, 661−670.

(11) Meyer, P. T., Bhagwagar, Z., Cowen, P. J., Cunningham, V. J., Grasby, P. M., and Hinz, R. (2010) Simplified quantification of 5-HT2A receptors in the human brain with [^{11}C]MDL 100,907 PET and non-invasive kinetic analyses. *NeuroImage 50*, 984−993.

(12) (a) Rosell, D. R., Thompson, J. L., Slifstein, M., Xu, X., Frankle, G., New, A. S., Goodman, M., Weinstein, S. R., Laruelle, M., Abi-Dargham, A., and Siever, L. (2010) Increased Serotonin 2A receptor availability in the orbitofrontal cortex of physically aggressive personality disordered patients. *Biol. Psychiatry 67*, 1154−1162. (b) Rylands, A. J., Hinz, R., Jones, M., Holmes, S. E., Feldmann, M., Brown, G., McMahon, A. W., and Talbot, P. S. (2012) Pre- and postsynaptic serotonergic differences in males with extreme levels of impulsive aggression without callous unemotional traits: A positron emission tomography study using 11C-DASB and 11C-MDL100907. *Biol. Psychiatry 72*, 1004−1011. (c) Talbot, P. S., Slifstein, M., Hwang, D., Huang, Y., Scher, E., Abi-Dargham, A., and Laruelle, M. (2012) Extended characterisation of the serotonin 2A 5-HT2A receptor-selective PET radiotracer 11C-MDL100907 in humans: Quantitative analysis, test-retest reproducibility, and vulnerability to endogenous 5-HT tone. *NeuroImage 59*, 271−285. (d) Jorgensen, C. V., Jacobsen, J. P., Caron, M. G., Klein, A. B., Knudsen, G. M., and Mikkelsen, J. D. (2013) Cerebral 5-HT2A receptor binding, but not mGluR2, is increased in tryptophan hydroxylase 2 decrease-of-function mice. *Neurosci. Lett.*, 118−122.